The effects of fuel type and cathode off-gas recirculation on combined heat and power generation of marine SOFC systems

van Veldhuizen, B. N.; van Biert, L.; Amladi, A.; Woudstra, T.; Visser, K.; Aravind, P. V.

DOI
10.1016/j.enconman.2022.116498

Publication date
2023

Document Version
Final published version

Published in
Energy Conversion and Management

Citation (APA)
van Veldhuizen, B. N., van Biert, L., Amladi, A., Woudstra, T., Visser, K., & Aravind, P. V. (2023). The effects of fuel type and cathode off-gas recirculation on combined heat and power generation of marine SOFC systems. *Energy Conversion and Management*, *276*, Article 116498. https://doi.org/10.1016/j.enconman.2022.116498

Energy Conversion and Management 276 (2023) 116498

Contents lists available at ScienceDirect

Energy Conversion and Management

journal homepage: www.elsevier.com/locate/enconman

The effects of fuel type and cathode off-gas recirculation on combined heat and power generation of marine SOFC systems

B.N. van Veldhuizen [a,*], L. van Biert [a], A. Amladi [b], T. Woudstra [b], K. Visser [a], P.V. Aravind [b]

[a] Department Ship Design, Production and Operations, Delft University of Technology, Mekelweg 5, 2628 CD Delft, The Netherlands
[b] Energy Conversion, Energy and Sustainability Research Institute, University of Groningen, Nijenborgh 6, 9747 AG Groningen, The Netherlands

ARTICLE INFO

Keywords:
Solid Oxide Fuel Cell
Ships
Alternative fuels
Thermodynamic analysis
Heat integration
Sustainability

ABSTRACT

An increasing demand in the marine industry to reduce emissions led to investigations into more efficient power conversion using fuels with sustainable production pathways. Solid Oxide Fuel Cells (SOFCs) are under consideration for long-range shipping, because of its high efficiency, low pollutant emissions, and fuel flexibility. SOFC systems also have great potential to cater for the heat demand in ships, but the heat integration is not often considered when assessing its feasibility. This study evaluates the electrical and heat efficiency of a 100 kW SOFC system for marine applications fuelled with methane, methanol, diesel, ammonia, or hydrogen. In addition, cathode off-gas recirculation (COGR) is investigated to tackle low oxygen utilisation and thus improve heat regeneration. The software Cycle Tempo is used to simulate the power plant, which uses a 1D model for the SOFCs. At nominal conditions , the highest net electrical efficiency (LHV) was found for methane (58.1%), followed by diesel (57.6%), and ammonia (55.1%). The highest heat efficiency was found for ammonia (27.4%), followed by hydrogen (25.6%). COGR resulted in similar electrical efficiencies, but increased the heat efficiency by 11.9% to 105.0% for the different fuels. The model was verified with a sensitivity analysis and validated by comparison with similar studies. It is concluded that COGR is a promising method to increase the heat efficiency of marine SOFC systems.

1. Introduction

The International Maritime Organisation (IMO) adopted a strategy in 2018 to decrease emissions by the marine industry. An aim of 40% carbon dioxide emission reduction by 2030 was set with respect to 2008 [1]. Moreover, limits on NO_X, SO_X and particulate matter (PM) emissions were introduced, which are even stricter in dedicated emission control areas [2]. Many alternative fuels (e.g., LNG, methanol, FT-diesel, ammonia, and hydrogen) are under consideration to reduce ship emissions [3]. However, using alternative fuels in marine engines is not a straightforward choice. Firstly, there are still significant NO_X emissions due to the combustion process. Secondly, the use of alternative fuels in internal combustion engines can cause lubrication, cooling, ignition, and knocking problems, introducing new challenges to combustion engine design [4,5]. Baldi et al. [6] identified Solid Oxide Fuel Cell (SOFC) systems as a promising technology for emission reduction in medium to long-distance ship applications. The efficiency of SOFCs exceeds internal combustion engines, while barely emitting NO_X and PM emissions [7]. Electrical efficiencies up to 60% have been reported for stand-alone cycles [8]. However, the application of SOFC systems in ships is still limited because of their low power density, high investment cost, limited lifetime, and slow response to dynamic loads. Nevertheless, fuel cell systems are characterised by good part-load characteristics, high redundancy, little maintenance, and low noise and vibrations, which are all beneficial for marine applications [9]. The high operating temperature of SOFCs offers flexibility in terms of fuel choice [10], which is perceived as a key aspect for the transition from fossil to renewable fuels in ships [11]. State-of-the-art SOFC systems can be fuelled with natural gas or hydrogen, but the conversion of ammonia, methanol, and diesel has also been positively evaluated with cell experiments [10]. However, it is not known which fuel could be converted most efficiently in marine applications.

1.1. Heat integration of SOFC systems

Many researchers investigated use of the high temperature outlets streams of SOFCs to further increase the conversion efficiency, for instance, with gas turbines [12], steam turbines [13], or ranking cycles [14]. Although many combined cycle studies predict high efficiency, it results in a more complex power plant with large control challenges and reduced part-load performance [7]. Ships often have a

* Corresponding author.
E-mail address: b.n.vanveldhuizen@tudelft.nl (B.N. van Veldhuizen).

https://doi.org/10.1016/j.enconman.2022.116498
Received 24 June 2022; Received in revised form 8 November 2022; Accepted 18 November 2022
Available online 8 December 2022

significant heat demand, which is usually met with exhaust gas recovery supported by fuel or electric boilers. Baldi et al. [15] demonstrated the significance of the heat demand in passenger ships, which can be over 25% of the total yearly energy demand. The exhaust streams of SOFCs contain much heat. Moreover, the waste heat recovery from conventional diesel generators is limited by a minimum exhaust gas temperature. The exhaust gas of sulphur-containing fuels should not be cooled below 150 °C, because the formation of sulphuric acid would corrode the exhaust system [16]. This means significant heat is present in the emitted exhaust gas. All in all, applying SOFC systems to ships fuelled with a sulphur-free fuel has the potential for high heat recovery. However, the heat integration is barely covered in studies into marine SOFC power plants [6].

1.2. Cathode off-gas recirculation

Cathode recirculation can be used to increase the heat efficiency of SOFC systems. Mehr et al. [17] and Chen et al. [18] proposed cathode off-gas recirculation (COGR) to preheat the inlet air of the SOFC, thus increasing the heat efficiency. Liso et al. [19] mentioned that the recycle loop reduces the primary airflow and thus reduces the air pre-heater dimensions. Air blowers can be used to recirculate the air and overcome the pressure loss of the SOFC [20]. However, the use of a high-temperature air blower introduces design challenges [21], and are not commercially available at operational temperatures above 300 °C [22]. Nevertheless, Tomberg et al. [23] recently demonstrated successful operation of a high-temperature blower in an anode recirculation configuration. Wang et al. [24] applied a low-temperature cathode recirculation loop to avoid the HT-COGR challenges, but cooling and reheating add to the thermal losses and system size. Alternatively, ejectors can recirculate the cathode off-gas [18], but they are difficult to control [25]. In the system analyses of Kazempoor et al. [26] and Jia et al. [27], the lower primary airflow due to COG-R increased the net electric efficiency due to a decrease in blower power, but no blower was used in the recirculation loop.

In the present paper, COGR is investigated to enhance the heat quality of the exhaust stream to improve the heat regeneration capacity for ship auxiliary systems. COGR reduces the primary airflow, which limits the amount of heat needed for air preheating and improves the air-fuel ratio in the combustor. This subsequently increases the temperature of the flue gas, which is beneficial for heat regeneration. Moreover, a smaller primary airflow is desirable in ships since it decreases the volume required for air and exhaust piping.

1.3. Objective & outline

This study compares the performance of a marine SOFC power plant for methane, methanol, diesel, ammonia, and hydrogen in terms of electrical and thermal efficiency. COGR is investigated with the aim of increasing the amount and quality of heat regeneration. The contributions of this paper are as follows:

1. One of the main novelties of this work is applying cathode off-gas recirculation to increase the heat recovery capacity in an application where heat can be used efficiently. The effects of COGR on oxygen utilisation and flue gas temperature are quantified. The study shows that COGR strongly increases the magnitude and quality of heat recovery and reduces the size of the air pre-heater. Evaluation of COGR for five different fuels showed that the benefits are the largest for methanol and hydrogen.
2. This paper provides a systematical comparison of the conversion efficiency of an SOFC power plant for five alternative marine fuels. Comparing existing studies with different fuels was not sufficient, because the results of other studies depend much on the system architecture and operational parameters of the SOFC.

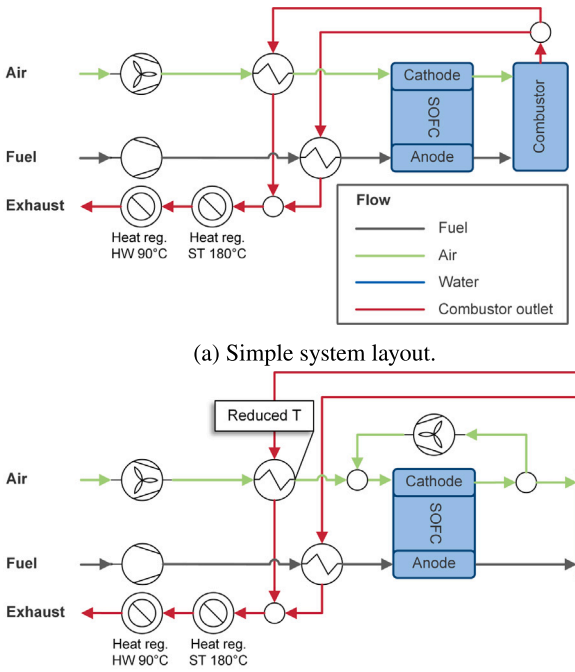

(a) Simple system layout.

(b) System layout with cathode off-gas recirculation.

Fig. 1. Reference SOFC systems.

3. In this research suitable system architectures for a marine SOFC power plant are generated for different fuels, taking into account the reforming process and efficient heat regeneration.
4. The validation section provides an extensive comparison of the present study with thermodynamic analyses of comparable systems. Besides validating the present study, this gives insight in what assumptions other researchers used and how it influenced their results.

The system designs for the selected fuels are described in Section 2. Potential fuels for marine SOFC systems have been selected in earlier research based on production capacity, stored energy density, technological readiness, safety, fuel cost, cost of the fuel storage system, and environmental impact [28]. Section 3 explains the thermodynamically modelling of the SOFC system. The results are presented in Section 4 with and without COGR. Verification and validation are provided in Section 5, by reflecting on the model limitations, analysing the model sensitivity, and comparing the results with comparable thermodynamic analyses. Conclusions are drawn in Section 6.

2. Description of selected SOFC systems

A general reference model is defined based on system configurations by Jia et al. [27], Kazempoor et al. [26], and Liso et al. [19], see Fig. 1(a). The fuel is supplied by a pump, compressor, or blower and is preheated before entering the anode. Air is supplied with a blower and preheated. Co-flow planar SOFCs converts the fuel into power and flue gas. The anode and cathode outlets flow directly into a combustor. Its exhaust leads through the counterflow heat exchangers that preheat the fuel and air. The flue gas flow is split to make sure the fuel and air can both reach the required temperature at the SOFC inlets. This is especially relevant for the carbon fuels, because additional heat is required at the fuel side, since steam is necessary to prevent carbon deposition and additional heat is needed for the reforming process. Finally, the remaining heat is recovered from the exhaust stream to the saturated steam net (180 °C at 9 bar) and the hot water net (90 °C at ambient pressure). These are common temperatures and pressures for

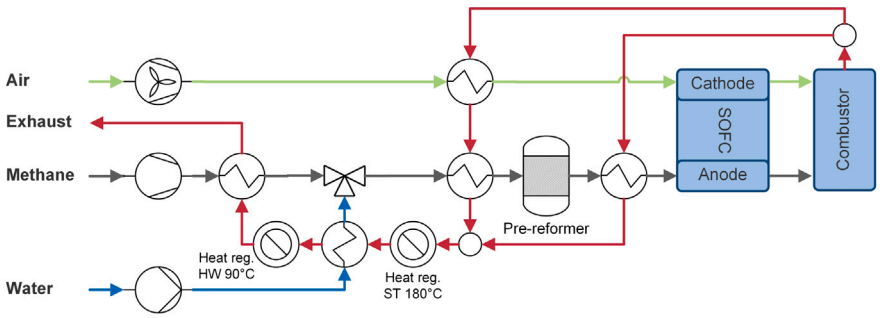

(a) Methane-fuelled SOFC system.

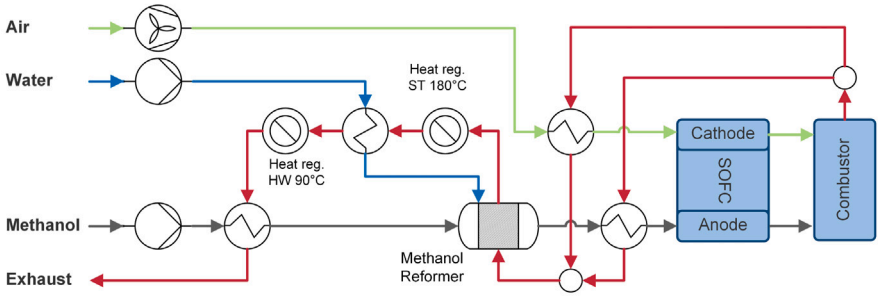

(b) Methanol-fuelled SOFC system.

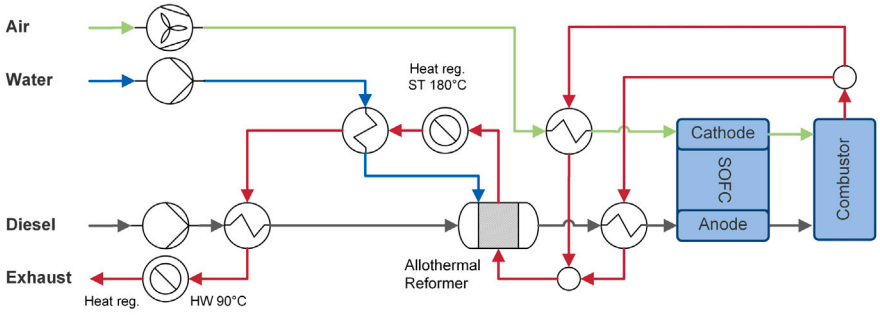

(c) Diesel-fuelled SOFC system.

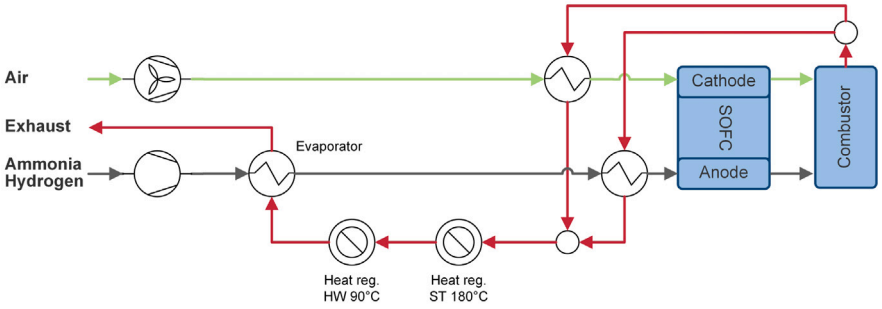

(d) Ammonia-fuelled SOFC system and hydrogen-fuelled SOFC system.

Fig. 2. SOFC system layout of SOFC for various fuels.

ship applications [16,29]. Additional components for the specific fuels (e.g., evaporators, reformers, and heat exchangers) are added in the order of required heat quality. For the COGR configuration, a variable air blower is used in the recirculation loop to control the recirculation ratio, see Fig. 1(b).

2.1. Methane system

The methane system layout is very similar to the configuration presented by Jia et al. [27], see Fig. 2(a). Methane steam reforming and the water gas shift (WGS) reaction convert part of the methane to a hydrogen-rich gas (Eqs. (1) and (2)). An adiabatic pre-reformer is applied to reduce stress on the fuel catalyst in the SOFC. The pre-reform ratio is defined in Eq. (3) [30]. Much internal reforming results in a higher net electric efficiency since less blower power is required for air cooling. For this reason, the minimum pre-reform ratio as stated by the SOFC supplier is used, which is 20%. The anode supply contains CH_4, H_2O, H_2, CO, and CO_2. Water is required for the reforming, which is heated and added as steam. A constant steam to carbon ratio (S/C) of 2.3 is used to prevent carbon deposition.

$$CH_4 + H_2O \rightleftharpoons CO + 3H_2 \quad (1)$$

$$CO + H_2O \rightleftharpoons H_2 + CO_2 \quad (2)$$

$$a_{PR} = 1 - \frac{\left(\chi_{CH_4} \cdot \dot{M}\right)^{out}_{reformer}}{\left(\chi_{CH_4} \cdot \dot{M}\right)^{in}_{reformer}} \quad (3)$$

where χ is the molar fraction and $\dot{M}$ the molar flow rate. An additional heat exchanger is added to the exhaust stream after the reformer, because the adiabatic pre-reformer reduces the fuel temperature. The exhaust stream is also used to generate the required steam. Since the fuel is usually stored cryogenically at −162 °C, remaining heat in the exhaust stream is used to evaporate and preheat the fuel.

2.2. Methanol system

Methanol is stored as a liquid at ambient temperature, so the methanol is supplied with a pump and evaporated by using heat of the exhaust stream, see Fig. 2(b). Xu and Ni [31] positively evaluated direct feed of methanol to SOFC, however, it is often concluded that extremely high temperatures are necessary for adequate methanol conversion [32,33]. In order to use comparable operational conditions to the other fuels, the methanol is decomposed in an external reformer (Eqs. (4) and (2)), similar to the configuration by Cocco and Tola [34]. It is assumed that the gaseous methanol is fully converted to H_2, H_2, CO, and CO_2. After the exhaust stream of the combustor preheats the fuel and air, heat is fed into the methanol reformer. Subsequently, heat is used for steam generation, hot water generation and finally to evaporate the methanol. The generated steam is fed to the methanol reformer.

$$CH_3OH \rightleftharpoons H_2 + CO \quad (4)$$

2.3. Diesel system

A diesel pump feeds preheated diesel into an allothermal reformer, see Fig. 2(c). Although, autothermal reformers are often considered in combination with SOFCs for being relatively compact in terms of size and weight, higher electric efficiencies can be reached with an allothermal reformer [35,36]. In this reformer, the diesel is converted to a hydrogen-rich gas with steam reforming (Eq. (5)) and WGS reaction. Similar to the methanol model, steam and exhaust heat are fed to the reactor.

$$C_nH_m + nH_2O \rightarrow (n + \frac{m}{2})H_2 + nCO \quad (5)$$

2.4. Ammonia system

The ammonia layout is based on the configurations of Farhad and Hamdullahpur [37] and Barelli et al. [38] and is shown in Fig. 2(d). The ammonia is evaporated, preheated and fed directly into the SOFC stack, where the ammonia is internally cracked (Eq. (6)). Direct feed of ammonia is mostly assessed at single cell level [39–41], but recently Barelli et al. [38] showed with stack experiments that external ammonia decomposition has a minimum influence on electric efficiency and is disadvantageous for the system size. They concluded that internal cracking is a feasible solution. All ammonia is converted because the operational temperature of the SOFCs is above 590 °C, the temperature of complete conversion [42]. Since ammonia is stored as a liquid at −33 °C, remaining heat is used to evaporate and heat up the fuel.

$$2NH_3 \rightleftharpoons N_2 + 3H_2 \quad (6)$$

2.5. Hydrogen system

The hydrogen system is similar to the basic system layout of Peters et al. [43]. The difference is that their configuration preheats the fuel with the anode off-gas instead of the flue gas, as was done by Sadeghi et al. [44]. Naturally, hydrogen is fed directly to the SOFC, see also Fig. 2(d). Similar to the ammonia system, remaining heat is used to evaporate and preheat the fuel from its liquid storage temperature (−253 °C).

Table 1
Used parameters for thermodynamic analysis.

General	Symbol	Value	Unit
Environment temperature	p_{amb}	25	°C
Environment pressure	T_{amb}	1.013	bar
SOFC			
Temperature both inlets	T^{in}_{SOFC}	680	°C
Temperature both outlets	T^{out}_{SOFC}	760	°C
Average cell temperature	T_{CELL}	720	°C
Pressure difference anode	Δp_{anode}	0.02	bar
Pressure difference cathode	$\Delta p_{cathode}$	0.015	bar
Nominal fuel utilisation	U_f	80%	–
Nominal cell voltage	V	0.8	V
Heat dissipation	Φ_{SOFC}	1.5	kW
DC-AC conversion	$\eta_{DC\|AC}$	0.96	–
Nominal AC power output	$P_{SOFC,AC}$	100	kW
Equipment			
Pressure loss across equipment	Δp	0.01	bar
Isentropic compressor efficiency	$\eta_{is,comp}$	0.7	–
Mechanical compressor efficiency	$\eta_{m,comp}$	0.8	–
Isentropic pump efficiency	$\eta_{is,pump}$	0.85	–
Mechanical pump efficiency	$\eta_{m,pump}$	0.6	–
Methane system			
Storage temperature	$T_{storage}$	−162	°C
Pre-reform ratio	a_{PR}	0.2	–
Steam reforming temperature	T_{reform}	725	°C
Steam to carbon ratio	S/C	2.3	–
Methanol system			
Reformer outlet temperature	T^{out}_{reform}	500	°C
Diesel system			
Reforming temperature	T_{reform}	540	°C
Ammonia system			
Storage temperature	$T_{storage}$	−33	°C
Hydrogen system			
Storage temperature	$T_{storage}$	−253	°C

3. Methodology

A flow-sheet software (Cycle-Tempo) is used for thermodynamic analysis of the fuel cell systems. Cycle-Tempo contains models for the relevant system components, such as pump, compressor, evaporator, reformer, fuel cell, combustor, and heat exchanger. Together, these components form a system matrix of mass and energy equations, which is used to calculate the mass flow, pressure, temperature and composition in all components. The ideal gas law and no losses in piping are assumed. The used parameters for the thermodynamic simulation are shown in Table 1.

3.1. SOFC model

The fuel cell and combustor use a Gibbs free energy minimisation routine to calculate the chemical equilibrium composition. In the SOFC model, the equilibrium compositions of the inlet gasses determine the electrical current and electrical power output, for which the internal temperature and pressures are assumed constant. Next, the required fuel flow for this current is calculated with the following equation [45]:

$$m^{in}_{an} = \frac{I \cdot M_{an}}{2F\left(y^{in}_{H_2} + y^{in}_{CO} + 4y^{in}_{CH_4}\right)U_F} \quad (7)$$

where m^{in}_{an} is the mass flow of the anode inlet, M_{an} is the molar mass of the anode gas, F is the Faraday constant and y^{in}_j the molar concentration of species j at the anode inlet, and U_F the fuel utilisation. A 1D model is used to calculate the current density, voltage and electrical power. This imposes the assumption that temperature, pressure and

gas composition are constant over the cross-section perpendicular to the fuel flow. Higher dimension models are more accurate, but they strongly increase the computational time and are most relevant for estimating the dynamic response of SOFCs [46]. Since this research focuses on steady-state operation, a 1D model is sufficient. The particle concentration, reversible voltage, and current density are calculated through the fuel cell stack as a function of position x. The reversible voltage at x is calculated with the Nernst equation [45]:

$$V_{rev,x} = V_{rev,0} + \frac{RT}{2F} \ln\left(\frac{\sqrt{y_{O_2,ca}} \cdot y_{H_2,an}}{y_{H_2O,an}} \cdot \sqrt{p_{cell}} \right) \tag{8}$$

where $V_{rev,0}$ is the standard reversible voltage, R the universal gas constant, T the temperature, and p_{cell} the cell pressure. The model assumes no voltage losses at the electrode in x direction, resulting in the following current density at x:

$$i_x = \frac{\Delta V_x}{R_{eq}} = \frac{V_{rev,x} - V}{R_{eq}} \tag{9}$$

with R_{eq} being the equivalent cell resistance. The current density depends on the fuel utilisation at position x, which is maximum at the inlet and zero at the outlet. The average current in the stack is shown in Eq. (10) [45]. The average current results from the integration of the local current densities over the dimensionless reaction coordinates λ, which represents the part of the fuel that already has been electrochemically converted.

$$I_{cell} = \frac{U_F \cdot V_{cell} \cdot A_{cell}}{R_{eq} \int_0^{U_F} d\lambda / \left(V_{rev,x} - V\right)} \tag{10}$$

where A_{cell} represents the cell area. Following, the power is directly calculated from the current and voltage. From the required electrical power and electrochemical balance, the required fuel flow is determined. The oxygen mass flow from the cathode to the anode is calculated using the determined current. Since the nominal inlet and outlet temperatures were defined, the flow through the cathode depends on the oxygen required for the reaction or the required cooling in the stack. The required cooling was in every case the determining factor for the cathode airflow.

Although SOFC stacks are well-insulated, some heat will dissipate into the environment. A constant heat dissipation Φ_{SOFC} of 1.5 kW is assumed, which resulted from steady-state testing. This assumption can be justified because the stack temperature is kept constant in all simulations in this research, as was done by Liso et al. [19].

3.2. Balance of plant components

It is assumed that the combustor converts all in-flowing combustible gases [7]:

$$\alpha H_2 + \beta CH_4 + \gamma CO + \left(\frac{\alpha}{2} + 2\beta + \frac{\gamma}{2}\right) O_2 \rightarrow (\alpha + 2\beta)H_2O + (\beta + \gamma)CO_2 \tag{11}$$

For compressors and pumps, the isentropic efficiency is used to estimate the actual power required for the pressure increase, compared with the amount of power required for ideal compression [47]. The isentropic and mechanical efficiency are assumed constant (see Table 1), and the values are based on literature with similar rated power [7,22]. The required power is calculated with Eq. (12) [7].

$$P_{comp/pump} = \dot{m} \frac{h_{out,is} - h_{in}}{\eta_m \cdot \eta_{is}} \tag{12}$$

where $h_{out,is}$ represents the enthalpy after isentropic pressure increase, η_m the mechanical efficiency of the equipment, and η_{is} the isentropic efficiency of the equipment.

3.3. Cathode recirculation system

For the SOFC systems with COGR, the recirculation ratio (RR) is defined as the mass flow in the circulation loop divided by the cathode outlet mass flow, see Eq. (13).

$$RR = \frac{\dot{m}_{recycle}}{\dot{m}_{ca}^{out}} \tag{13}$$

The recirculation rate affects the overall oxygen utilisation in the SOFC system, which in this paper excludes the combustion process:

$$(U_O)_{overall} = 1 - \frac{\left(\chi_{O_2} \cdot \dot{M}\right)_{combustor}^{in}}{\left(\chi_{O_2} \cdot \dot{M}\right)_{airblower}^{in}} \tag{14}$$

where χ is the molar fraction and $\dot{M}$ the molar flow rate. Peters et al. [48] consider oxygen utilisation above 50% to be infeasible, because a high oxygen utilisation reduces the equilibrium potential due to a lower molar oxygen concentration, see Eq. (8). Ni et al. [49] mentioned 20% as a suitable oxygen utilisation. In this study, the recirculation is set such that the temperature after the combustor does not exceed 900 °C. This limit is used to enable the use of gas-to-gas metal heat exchangers for air and fuel pre-heaters [50], and was also applied by Cinti et al. [51] and Liso et al. [19].

3.4. System performance

After subtracting the parasitic electrical power losses and converting DC to AC power, the net electrical efficiency of the SOFC system is based on the lower heating value [17]:

$$\eta_{net,AC} = \frac{\eta_{DC|AC} P_{SOFC,DC} - P_{aux}}{\dot{m}_{f,in} \cdot LHV_f} \tag{15}$$

where $\eta_{DC|AC}$ represents the electrical conversion efficiency from direct current to alternating current, $P_{SOFC,DC}$ the electrical power generated by the fuel cells, P_{aux} the parasitic power of pumps, blowers and compressors, $\dot{m}_{f,in}$ the mass flow of the dedicated fuel f, and LHV_f the lower heating value of fuel f.

Remaining heat in the exhaust stream is recovered for the hot water (HW) and saturated steam (ST) network with a pinch point temperature of 10 °C. Subsequently, for the saturated steam network, heat is subtracted from the exhaust stream up to 190 °C. For the hot water network, heat is subtracted from the exhaust stream up to 100 °C. The amount of regenerated heat for hot water and saturated steam determines the heat efficiency:

$$\eta_{heat} = \frac{\dot{Q}_{HW} + \dot{Q}_{ST}}{\dot{m}_{f,in} \cdot LHV_f} \tag{16}$$

with $\dot{Q}$ being the heat flow that is recovered from the exhaust stream. Heat exchangers are usually bulky and expensive equipment and their size and cost strongly depend on the required heat transmission [19]. Deviations in mass flow influence the amount of transferred heat. Moreover, a higher flue gas temperature positively influences the heat transfer rate. The differences in heat exchanger size for the different fuels and for employing COGR are taken into account in the performance evaluation. The increase in heat exchanger surface area is estimated with the often used LMTD method, see Eqs. (17) and (18) [52]. This method assumes no heat loss to the surroundings, steady flow conditions, constant specific heat, and constant overall heat transfer coefficient.

$$A_S\ [\%] = \frac{\left(\dot{Q}/LMTD\right)_{COGR}}{\left(\dot{Q}/LMTD\right)_{no\ COGR}} \tag{17}$$

$$LMTD = \frac{\Delta T_1 - \Delta T_2}{\ln\left(\Delta T_1 / \Delta T_2\right)} \tag{18}$$

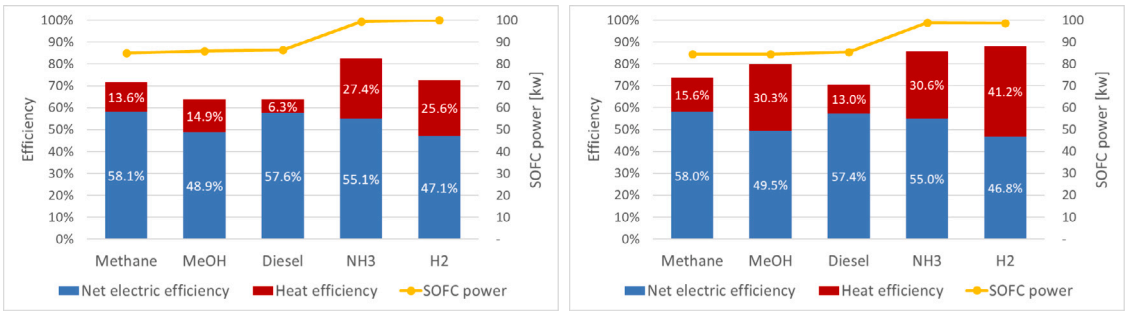

(a) Without COGR (b) With COGR

Fig. 3. Net electrical efficiency, heat efficiency and delivered SOFC power for the five selected fuels. Data is generated at nominal operation ($V = 0.8$ V and $U_F = 80\%$).

Table 2
Used parameters for simulations of all fuels.

Simulation	Fuel utilisation –	Cell voltage V	RR –
Nominal	80%	0.8	–
Operating range	70%–85% $\Delta = 1\%$	0.6–0.85 $\Delta = 0.01$	–
COGR	80%	0.8	0–0.77 $\Delta = 0.002$

4. Results

The results are generated by simulating the presented model with the parameters stated in Table 2. The main results regarding the electrical and heat efficiency for the considered fuels without COGR are presented in 3(a) and with COGR in 3(b). The results without COGR will be discussed in Sections 4.1 and 4.2 and the effect of COGR will be discussed in Section 4.3.

4.1. Electrical and heat efficiency

Fig. 3(a) compares the net electrical efficiency, thermal efficiency, and delivered AC power for the different SOFC systems. Methane, diesel, and ammonia resulted in high electrical efficiency. The electrical efficiency for methanol and hydrogen was much lower.

In the presented model, the heat efficiency is defined by the amount of heat that was regenerated for hot water and saturated steam purposes. Subsequently, the heat efficiency depends on the temperature and mass flow of the flue gas and the heat extraction by other components. The diesel-fuelled SOFC system had the lowest heat efficiency. This can be explained by a high heat consumption by the diesel reforming process. Ammonia resulted in the highest heat efficiency, because the ammonia is cracked internally. Moreover, the relatively small airflow resulted in high flue gas temperatures. It must be noted that not all supplied heat was of the same quality. Although hydrogen resulted in high heat efficiency, the temperature of the exhaust stream after fuel and air pre-heating was not sufficient to produce saturated steam.

For the carbon-containing fuels (methane, methanol, and diesel), the power density and thus delivered power was lower than for hydrogen and ammonia, which is illustrated with the yellow line in Fig. 3(a). Since the equivalent cell resistance, temperature, and cell pressure were assumed constant, the differences in power density can be explained by differences in species concentrations through the cell, influencing the reversible voltage, see Eqs. (8) and (9). Although the methane-fuelled system resulted in the highest electrical efficiency, the delivered power was 15% lower than when fuelled with ammonia or hydrogen. This implies more modules would need to be installed to deliver the same power.

4.2. Oxygen utilisation and blower losses

SOFCs are cooled with cathode air. The temperature difference between the cathode inlet and outlet was limited to 80 °C to prevent stress from large thermal gradients. Consequently, the required cooling determined the airflow and thus, the oxygen utilisation, which was generally much larger than the stoichiometric requirements. Large differences were found in the oxygen utilisation and required airflow for the different fuels. This can be explained by heat release differences in the electrochemical and reform reactions in the SOFC for the different fuels. Since the air blower was amply the largest contributor to the parasitic power consumption, oxygen utilisation had a significant impact on the net electrical efficiency. Fig. 4 shows the net electrical efficiency and the used air blower power over the delivered SOFC power, both as a function of oxygen utilisation. The oxygen utilisation reached fairly low values down to 5%, especially for methanol and hydrogen. For low oxygen utilisation, a large share of the generated power was demanded by the blower, which reduced the net electrical efficiency.

4.3. Effect of cathode off-gas recirculation

Cathode off-gas recirculation is employed to improve the heat regeneration from the exhaust stream. This section investigates the impact of the amount of recirculated air and evaluates the SOFC system with and without COGR.

4.3.1. Varying the recirculation ratio

Fig. 5(a) shows the impact of the recirculation ratio (RR) on the overall oxygen utilisation. As was expected, a high recirculation rate strongly increased the overall oxygen utilisation. For the methane, ammonia, and diesel system, the overall oxygen utilisation became particularly high (over 30%) when using recirculation ratios of 0.5 or higher.

Cathode recirculation has additional advantages for the SOFC system. Reducing the primary airflow lowers the required heat transfer in the air pre-heater. The transmitted heat in the air pre-heater exceeded the other heat exchangers by a factor of ten for the considered systems. Consequently, the air pre-heater was the largest and costliest heat exchanger in the system design. The striped lines in Fig. 5(a) show that the required heat transfer in this heat exchanger decreased linearly for an increasing cathode recirculation ratio. Large reductions in the required heat transfer were found, especially for the hydrogen and methanol system.

The striped lines in Fig. 5(b) show that a higher recirculation ratio increased the temperature in the exhaust stream. This increased the heat transfer potential for heat recovery. Despite the decrease in flow rate of the flue gas this positively affected the heat efficiency for all different fuels, which is shown with the solid line in Fig. 5(b).

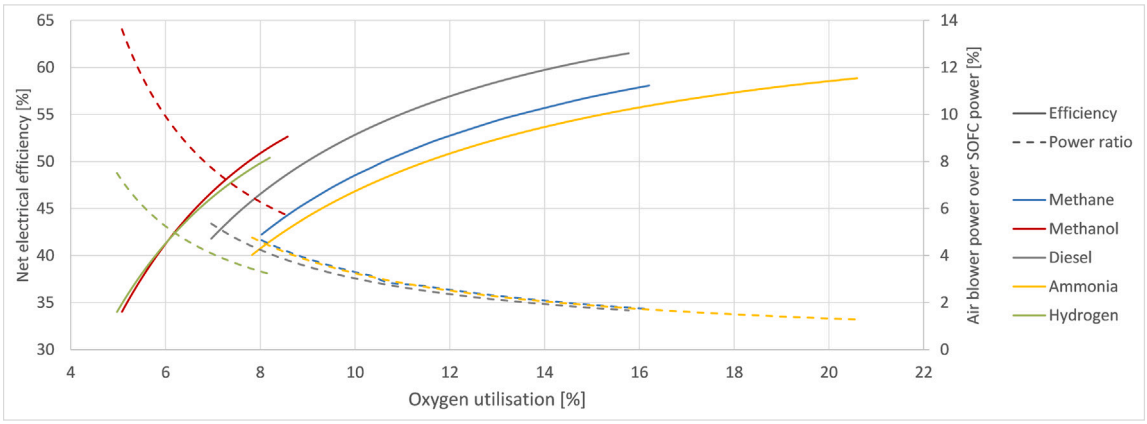

Fig. 4. Net electrical efficiencies and compressor power divided by delivered AC SOFC power, both plotted as function of the oxygen utilisation for the five selected fuels. Data is generated at $V = 0.6$–0.85 V and $U_F = 80\%$.

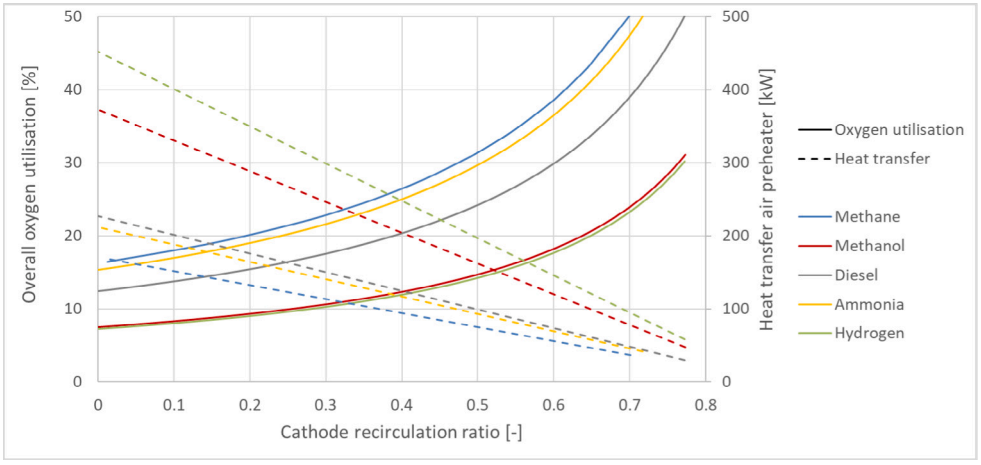

(a) Effect of RR on overall oxygen utilisation and heat transfer in air pre-heater. The oxygen utilisation does not include the consumed oxygen in the combustion process. A higher cathode recirculation, reduces the overall oxygen utilisation, which is accompanied by a lower primary airflow, and ultimately decreases the heat transfer in the air pre-heater.

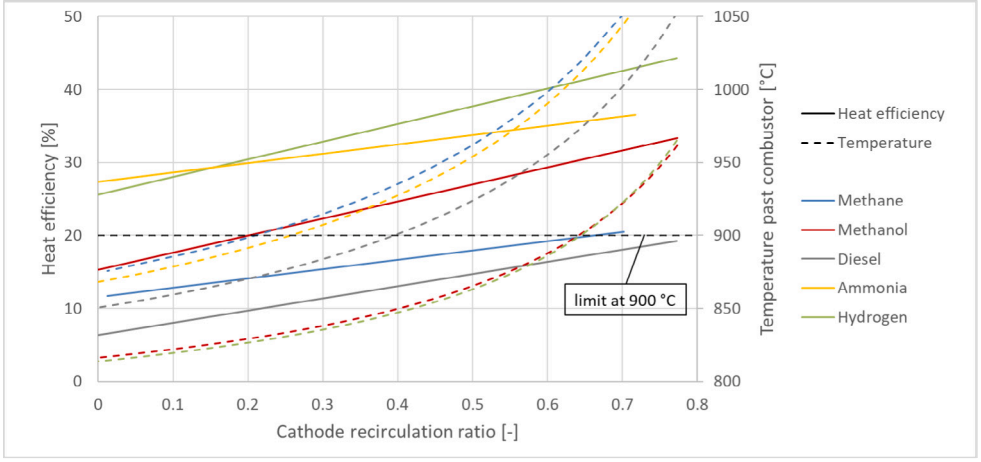

(b) Effect of RR on heat efficiency and flue gas temperature past the combustor. A higher cathode recirculation rate decreases the primary airflow, which increases the flue gas temperature. This ultimately leads to a higher heat efficiency, because more heat can be recovered from the flue gas.

Fig. 5. Impact of cathode off-gas recirculation ratio for different fuels at a cell voltage of 0.8 V, 80% fuel utilisation, and oxygen utilisation up to 50%.

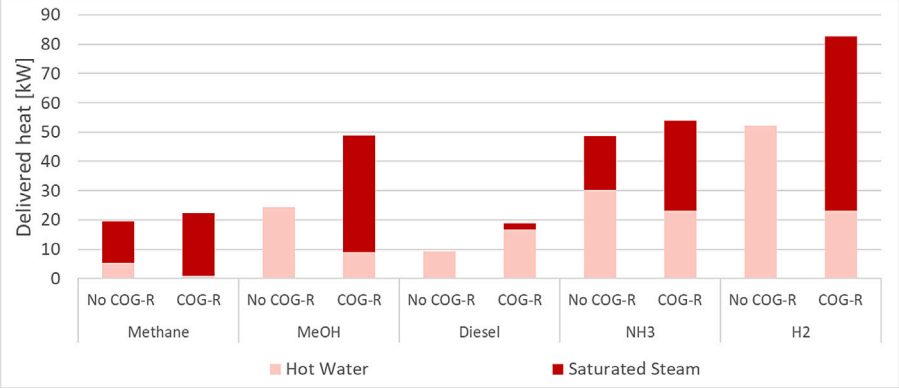

Fig. 6. Delivered heat to hot water and steam net for original systems and systems including cathode of gas recirculation (COGR). Data is generated at nominal operation ($V = 0.8$ V and $U_F = 0.8$).

Table 3
Influence of cathode off-gas recirculation on oxygen utilisation and system performance for different fuels at a cell voltage of 0.8 V and 80% fuel utilisation. The recirculating rate is maximised towards an upper limit by introducing a maximum flue gas temperature of 900 °C.

	Without COGR	*With COGR*			*Difference*			
	U_O	RR	Single pass U_O	Overall U_O	U_O	Elec. efficiency	Heat efficiency	Total efficiency
Methane	16.2%	19.6%	16.7%	20.0%	1.2×	−0.1%	+14.9%	+2.7%
Methanol	7.5%	64.3%	8.3%	20.3%	2.7×	+1.2%	+103.3%	+25.1%
Diesel	12.4%	39.8%	13.3%	20.3%	1.6×	−0.3%	+106.4%	+10.2%
Ammonia	15.4%	26.7%	16.0%	20.3%	1.3×	−0.1%	+11.9%	+3.9%
Hydrogen	7.2%	64.2%	8.0%	19.6%	2.7×	−0.8%	+61.0%	+21.0%

Table 4
Airflow and heat transfer for air pre-heater for SOFC system without and with COGR for different fuels, at a cell voltage of 0.8 V and 80% fuel utilisation. Difference in surface area is estimated with LMTD method.

	Without COGR	*With COGR*	*Difference*			
	Transmitted heat kW	Transmitted heat kW	Primary airflow –	Transmitted heat –	LMTD –	Surface area –
Methane	171	133	−19.1%	−21.9%	+22.1%	−36.1%
Methanol	373	101	−64.0%	−72.8%	+170.8%	−90.0%
Diesel	227	125	−39.3%	−44.9%	+62.0%	−66.0%
Ammonia	211	151	−25.2%	−28.5%	+32.0%	−45.8%
Hydrogen	451	124	−63.7%	−72.6%	+175.1%	−90.0%

4.3.2. With or without COGR

Table 3 shows the recirculation rates when the temperature in the exhaust stream is kept under 900 °C. Although the recirculation ratio varied much per fuel, the 900 °C limit resulted for all fuels in an overall oxygen utilisation of around 20%.

Fig. 3(b) shows the net electric efficiency, thermal efficiency, and delivered AC power for the different SOFC systems when COGR is applied with the exhaust temperature limit. Comparing Figs. 3(a) and 3(b) shows that employing COGR increased the heat efficiency by 11.9 to 105.0% for the different fuels. The large increase in thermal efficiency for methanol and hydrogen can be explained by a large increase in oxygen utilisation, which reduced the amount of preheated air. Table 3 displays a 2.7 times increase in oxygen utilisation in the system for methanol and hydrogen, for the other fuels this factor is just 1.2 to 1.6. Besides the increase in thermal efficiency, an improvement in the heat regeneration quality of the exhaust stream can be observed in Fig. 6. For the methanol and hydrogen system without COGR, the quality of the remaining heat after fuel and air preheating was not sufficient to generate any saturated steam. COGR strongly increased the amount of available heat for saturated steam purposes due to a higher flue gas temperature after heat subtraction for fuel and air, especially for the methanol and hydrogen system. A large take-off capacity for saturated steam (dark red in graph) is beneficial, since a surplus of heat can be bypassed and used for the hot water demand, but not vice versa.

The differences in net electric efficiency were minor. The power used by the air blower for the systems without COGR was approximately equal to the used power by the combined primary air blower and the recirculation blower. Moreover, a change in the single-pass oxygen utilisation in the stack only leads to small deviations in the stack's current density. All in all, the addition of COGR resulted in an increase in the total efficiency of 2.7% to 25.1% for the different fuels.

Table 4 shows the accomplished decrease in primary airflow and transmitted heat in the air pre-heater for COGR using the 900 °C flue gas limit. Moreover, the increase in flue gas temperature positively influenced the heat transfer rate in the air pre-heater. Employing COGR reduced the surface area of the heat exchanger by 36.1% to 90% for the various fuels. Consequently, COGR positively affected the size, weight, and cost of the SOFC system.

5. Discussion

This section reflects some of the assumptions in the thermodynamic analysis and discusses why these were made. Furthermore, the model is verified and the results are validated with earlier research.

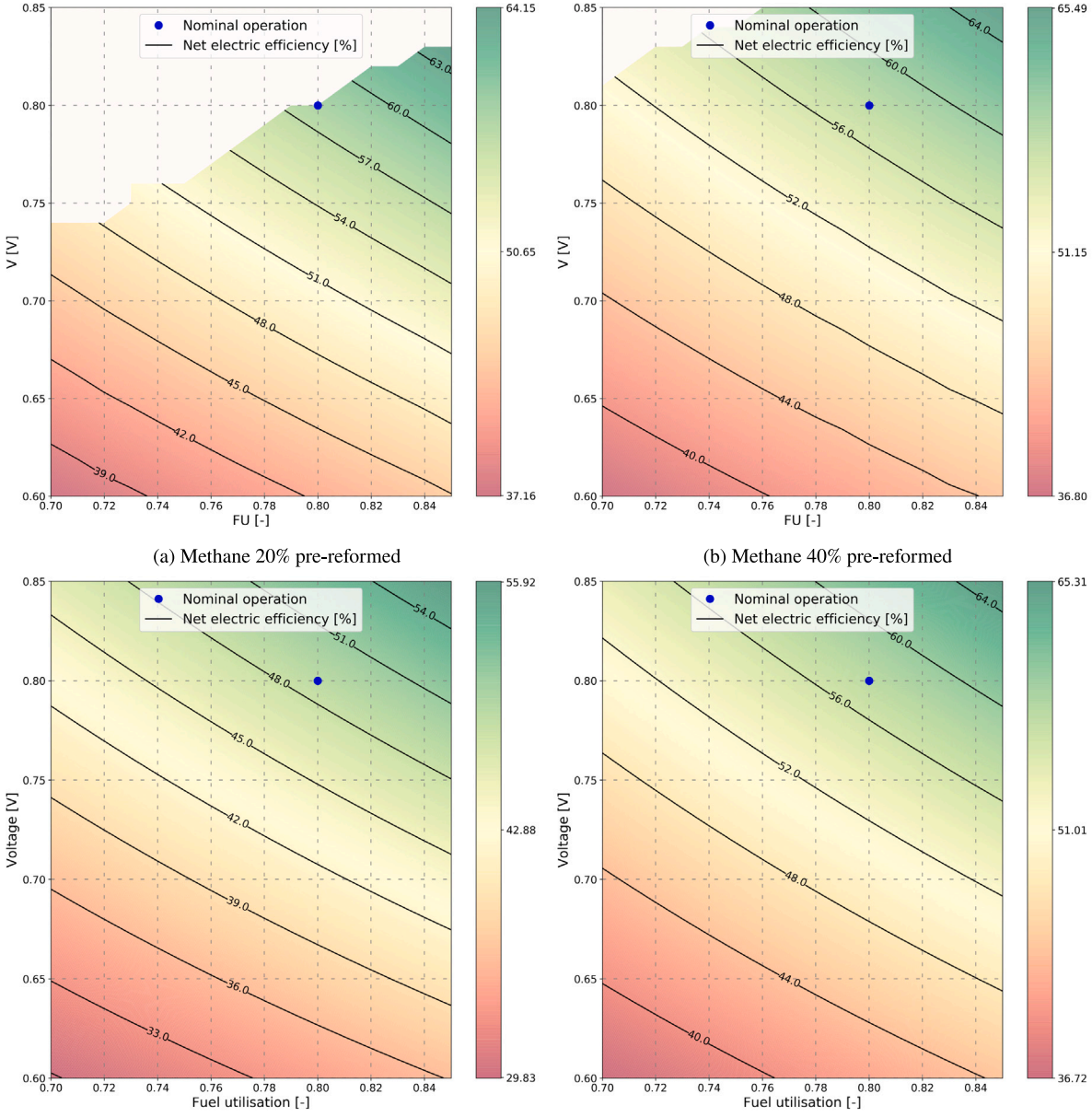

Fig. 7. Net electrical efficiency for systems without COGR at cell voltages of 0.6–0.85 V and fuel utilisation of 70–85%.

5.1. Model limitations

During the thermodynamic modelling, several assumptions were made:

- The cell resistance R_{SOFC} is kept constant for different fuels, voltages and fuel utilisation values, because of the unavailability of experimental data for all considered fuels with the same cell architecture. This assumption only holds if the thermal balance in the stack does not change significantly. Although the temperatures of the inlets and outlets stay equal, it could be argued that internal reforming significantly influences the thermal balance in the stack. The kinetics of the electrochemical and reforming reaction are affected by the local temperature and partial pressure of reactants. However, as both reactions in turn affect the spatial distributions of temperature and partial pressures, they are strongly coupled [53]. Nevertheless, this assumption is necessary to fairly compare the performance of the SOFC system for the selected fuels.
- The SOFC model does not consider activation, ohmic, and concentration losses separately, but includes the losses as an average. Activation losses dominate at low current densities and concentration losses start to dominate at high current densities. However, it can be assumed that the presented average loss characteristic is still representative since the SOFC operates in the ohmic region of the polarisation curve for the used input ranges of voltage (0.6–0.85 V) and fuel utilisation (70%–85%).
- Although the SOFC is operated at different voltages, the effectiveness deviations of the balance of plant components at different operational conditions are not included. For instance, air blowers operate at significantly lower efficiency below their operational speed. For most balance of plant components, this has a rather small influence on the net electric efficiency. However, Fig. 4

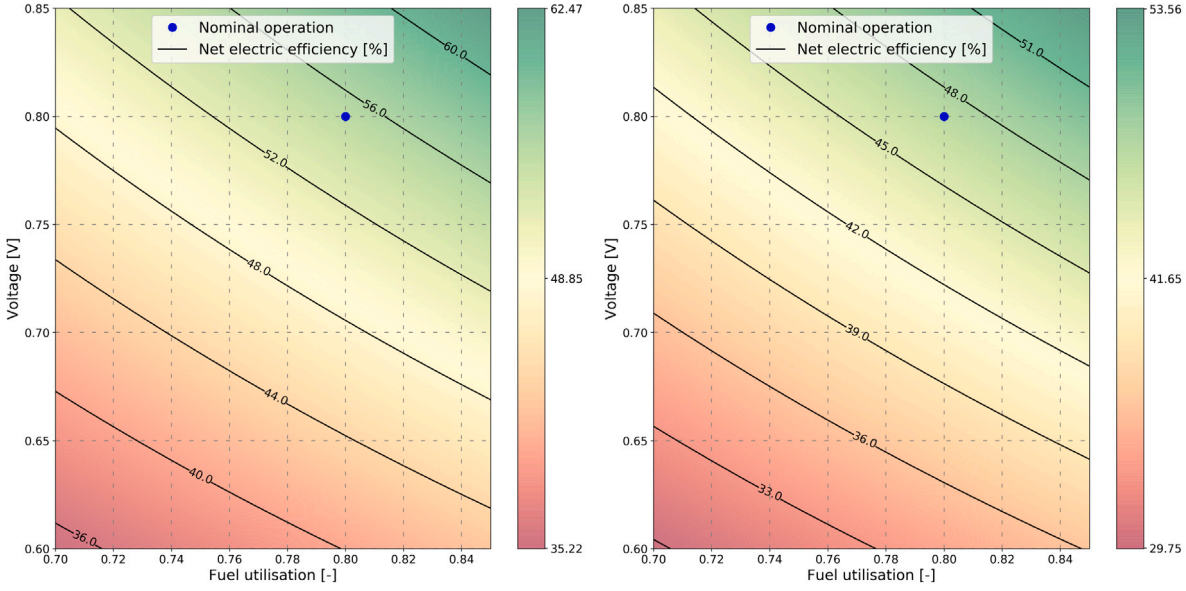

(a) Ammonia (b) Hydrogen

Fig. 8. Net electrical efficiency for systems without COGR at cell voltages of 0.6–0.85 V and fuel utilisation of 70–85%.

shows that the contribution of the air blower to the net electric efficiency is significant. Nevertheless, several configurations and operational modes were investigated for the nominal operation of a marine SOFC system. Different system configurations would require different operational designs of the balance of plant components to ensure they operate as much as possible in their operational conditions. Consequently, this assumption holds for the steady-state operation in this research. When the research would be extended to part-load operation, it would be necessary to include the part-load efficiency of at least the air blower.

- Heat loss in piping and components besides the SOFC are neglected. This is a widely used assumption in SOFC system analyses [54,55]. Although the system would be well insulated, in practice, some heat would still dissipate. Becker et al. [56] assumed fixed heat loss as a percentage of LHV for reformer, combustor, and piping, which was estimated at only 1.5%. Hollmann et al. [22] estimated significant heat losses by modelling all geometric and insulation properties in ANSYS. However, they argued that the high heat losses were caused by separate insulation of all components to ensure quick accessibility during testing and would be less significant in a commercial system.
- Pressure losses across all BOP components are simplified by assuming a constant pressure drop as was done by Liso et al. [19], which is well-accepted in thermodynamic analyses. An underestimation of the pressure drop across equipment could to an overestimation of the net electrical efficiency, because more parasitic power would be necessary for compressors or pumps. Some researchers formulate the pressure drop as function of the mass flow and a pressure drop correlation parameter [48,57]. However, the influence on the net electric efficiency is minor and Tan et al. [58] even neglect pressure drop across equipment. The assumption that the pressure drop in piping is negligible is widely used [44] and is valid because the distance between all components is short [19].

5.2. Model verification

A sensitivity analysis is performed for the operational conditions of the SOFC to verify whether the model behaves similar to a real SOFC system according to methods provided by Sargent [59]. The voltage and fuel utilisation are varied from 0.6 to 0.85 and 70% to 85%, respectively, see Figs. 7 and 8. The results are in line with theory and other thermodynamic analyses for all modelled systems. The net electrical efficiency increases for higher fuel utilisation and voltages, within the operational constraints of the SOFCs. Naturally, the highest electrical efficiency is also accompanied by the lowest current density.

The net electrical efficiency of the SOFC system is approximately linear to the voltage as to the fuel utilisation, since the stated ranges are in the ohmic region of the polarisation curve of the SOFC. Apparently, the other components in the system do not influence the system efficiency sufficiently to deviate much from this linear SOFC relation, taking into account that part-load effectiveness of the balance of plant components is not included.

The sensitivity analysis showed that the methane-fuelled system was not feasible for higher voltages, see Fig. 7(a). At higher voltages (i.e., lower current density), less heat is produced in the stack. Heat is required for the internal reforming of methane, and for high voltages, this results in a heat deficit in the SOFC. The pre-reform ratio could be increased to reduce the required heat in the stack and consequently improve the operational range of the stack. This is shown in Fig. 7(b) for a pre-reform ratio of 40%. Although this results in a slight reduction in electrical efficiency and a significant reduction in heat efficiency at equal operational conditions, the operational range is widened. The small decrease in net electrical efficiency is the consequence of a decrease in the endothermic internal reforming, which increases the cooling requirement by the cathode air, subsequently increasing the parasitic power of the blower [19,60]. For the other fuels, the SOFC system is feasible over the full considered operational range, see Figs. 7(c) to 8(b).

5.3. Result validation

The results are validated by comparison with other research. Specifically, the net electrical efficiency, since the actual heat efficiency is not often stated and depends much on the defined temperature at which heat regeneration is deemed feasible. The net electric efficiencies are as much as possible compared with research using similar process design, plant size, and SOFC operating conditions. Although some significant

Table 5
Comparison of SOFC system analyses without COGR. Only comparable studies are included, which means planar O^{2-} conducting SOFCs operated on atmospheric pressure. All efficiency data is based on LHV.

Fuel	Reference	*SOFC operation*		*Performance*
		Voltage V	Fuel utilisation –	Net electric efficiency –
Methane	Kazempoor et al. [26]	0.7	80%	49.5%
	Liso et al. [19]	?	80%	61.0%
	Jia et al. [27]	?	85%	41.0%
	Mehr et al. [17]	0.62	85%	41.8%
	Ahmadi et al. [62]	?	80%	47.8%
	This study	0.80	80%	58.1%
	This study	0.80	80%	57.7%
Methanol	Sangtongkitcharoen et al. [63]	0.62	80%	45.0%
	Cocco and Tola [34]	?	85%	50.0%
	Leone et al. [33]	?	80%	51.0%
	Rokni [64]	?	80%	51.9%
	This study	0.80	80%	48.9%
Diesel	Ezgi et al. [65]	0.80	90%	55.3%
	Nehter et al. [66]	0.75	73%	55.0%
	Huerta et al. [21]	0.75	85%	56.0%
	This study	0.80	80%	57.6%
Ammonia	Farhad and Hamdullahpur [37]	0.73	80%	41.0%
	Rokni [64]	?	80%	51.8%
	Cinti et al. [51]	?	80%	55.0%
	Barelli et al. [38]	0.78	80%	52.1%
	Selvam et al. [67]	0.855	80%	59.8%
	This study	0.80	80%	55.1%
Hydrogen	Kazempoor et al. [26]	0.78	80%	37.5%
	Botta et al. [68]	0.75	75%	40.0%
	Peters et al. [43]	0.86	80%	48.0%
	Sadeghi et al. [44]	0.85	85%	49.6%
	This study	0.80	80%	47.1%

General: – = Not applicable, ? = Not reported by author.

discrepancies were found, they can all be explained by differences in operating parameters or model assumptions. The comparison is, without and with COGR, summarised in Tables 5 and 6, respectively. An extensive comparison is provided in Tables 7 and 8 in the Appendix. Here, the main parameters that influence the net electrical efficiency are also listed, which are voltage, current density, fuel utilisation, stack temperature, blower efficiency, and inverter efficiency [60]. Moreover, the Appendix shows which systems use anode off-gas recirculation (AOGR). AOGR is often proposed to increase the electrical efficiency and reduce the steam generator requirements, and can be used in combination with COGR [61].

5.3.1. Methane

Liso et al. [19] studied natural gas-based combined heat and power (CHP) systems in various configurations. When using steam reforming and no recirculation streams, they found a net electrical efficiency of 61% for a pre-reform ratio of 40%. This is similar to the 58% electrical efficiency found in the present study for the same pre-reform ratio, see Fig. 7(b). The stack temperature is also similar in both studies (750 °C and 720 °C). Other studies have also found various electrical efficiencies within the range of this study, which is 37% to 65% for voltages from 0.6 to 0.85 V. In a thermodynamic analysis for residential applications using 30% pre-reforming and 60% anode off-gas recycling, Kazempoor et al. [26] simulated a net electrical efficiency of 49.5% at 0.7 V and 80% fuel utilisation. Using direct internal reforming and no recirculation, Jia et al. [27] found 41% electrical efficiency at 85% fuel utilisation, but the operating voltage is not given. Without employing a pre-reformer, Mehr et al. [17] found a much lower electrical efficiency (exergy) of 41.8% at 85% fuel utilisation, but the fuel cell was operated at 0.62 V. Ahmadi et al. [62] simulated a CHP plant without a pre-reformer, operating at a lower temperature (640 °C) and 80% fuel utilisation, which resulted in a net electrical efficiency of 47.8%.

Opposed to this study, in the work of Liso et al. [19], Kazempoor et al. [26] and Jia et al. [27] the net electrical efficiency strongly improved when COGR was applied, which was a direct consequence of a smaller air blower power. However, in their studies, no blower was used in the recirculation loop, which explains the difference from the present study. Wang et al. [24] studied energy storage systems using reversible solid oxide cells using cathode off-gas recirculation. Their net electrical efficiency ranged from 60.2% to 62.4% for current densities of 4000 to 3000 A/m^2, which is slightly higher than 58.0% at 3465 A/m^2 in this study. This can be explained since the cathode is fed with pure oxygen, which results in a smaller airflow and thus a lower blower power.

5.3.2. Methanol

Cocco and Tola [34] studied an SOFC-GT system fuelled by methanol. Although combined cycle systems often result in higher efficiencies, the SOFC efficiency was reported separately at 50%. This is similar to the nominal electrical efficiency found in the present study, which is 49%. Leone et al. [33] thermodynamically analysed a CHP SOFC plant, which also resulted in a very similar efficiency of 51% at 80% fuel utilisation. Wang et al. [24] have again reported higher efficiencies in the range of 54% to 64%, compared with 30% to 55% in the present study. Sangtongkitcharoen et al. [63] found a lower net electrical efficiency of 45% for a reformed methanol-fuelled SOFC at similar fuel utilisation and current density as the present study. This difference can be explained, since they operated the SOFCs on 0.62 V. Although Rokni [64] employed a methanator and anode off-gas recirculation with an RR of 3%, their net electrical efficiency (51.9%) was still very similar to the present study.

5.3.3. Diesel

Most studies on diesel-fuelled SOFC systems report electric efficiencies similar to the present study (58%). Ezgi et al. [65] thermodynamically modelled an SOFC system for auxiliary power generation on a naval ship using autothermal reforming. They reported an electrical efficiency of 55.3% at the same voltage as our study (0.8 V) and a slightly higher operating temperature of 775 °C. The slightly lower electrical efficiency at even higher temperatures can be explained by the use of autothermal reforming. Nehter et al. [66] and Huerta et al. [21] both use steam reforming and anode off-gas recirculation, reporting efficiencies of 55% and 56% respectively at a slightly lower voltage of 0.75 V.

5.3.4. Ammonia

Cinti et al. [51] studied an ammonia-fuelled system with internal cracking. At an operating temperature of 750 °C and fuel utilisation of 80%, they found net electric efficiency in the range of 38% to 67% depending on the power output. This is similar to the range found in the present study (35% to 62%) for similar operating conditions Rokni [64] and Selvam et al. [67]. Also found efficiencies in the same range. The results of Barelli et al. [38] were most in line with the present study, they found a net electrical efficiency of 52.1% at a slightly lower voltage (0.78 V) compared with 55.1% at 0.8 V of the present study. Their model was also validated with short stack experiments. Farhad and Hamdullahpur [37] studied a portable power system with a similar process design as this study. They found an efficiency of 41% at a voltage of 0.73 V and a fuel utilisation of 80%. Under the same conditions, the present study found an efficiency of around 50%, see Fig. 8(a). In the study of Farhad and Hamdullahpur [37], 20% parasitic power take-off was assumed for the control system since it is only a small system (100 W) and DC power is delivered. Together, this explains the 18% difference in net electrical efficiency compared with

Table 6
Comparison of SOFC system analyses with COGR. Only comparable studies are included, which means planar O^{2-} conducting SOFCs operated on atmospheric pressure. All efficiency data is based on LHV. For diesel and ammonia, no representative studies with COGR were found.

Fuel	Reference	*SOFC operation*				*Performance*
		COGR type –	COG RR –	Voltage V	Fuel utilisation –	Net electric efficiency –
Methane	Kazempoor et al. [26]	EJ	0.6	0.69	80%	53.7%
	Liso et al. [19]	EJ	0.75	0.80	80%	58.0%
	Jia et al. [27]	?	0.5	?	85%	51.0%
	Mehr et al. [17]	?	0.3	0.60	85%	40.2%
	Wang et al. [24]	BL	?	0.83	90%	65.9%
	This study	BL	0.2	0.80	80%	58.0%
Methanol	Wang et al. [24]	BL	?	0.83	90%	60.2%
	This study	BL	0.64	0.80	80%	49.5%
Hydrogen	Kazempoor et al. [26]	EJ	0.6	0.78	80%	40.3%
	Wang et al. [24]	BL	?	0.859	90%	58.3%
	This study	BL	0.64	0.80	80%	46.8%

COGR type: BL = Air recirculation with blower, EJ = Air recirculation with ejector.

the present study. Wang et al. [24] used an external cracker and pure oxygen to feed the cathode, finding net electric efficiency in the range of 58.2% to 61.6% for current densities of 4000 to 3000 A/m^2. This again is significantly higher than 55.1% at 4075 A/m^2 of the present study.

5.3.5. Hydrogen

The present study found electrical efficiencies in the range of 30% to 53% for a fuel utilisation of 80% and a stack temperature of 720 °C, with a nominal efficiency of 47.1% at 0.8 V. Botta et al. [68] have found an energy efficiency of 40% at an average cell temperature of 850 °C but at a lower fuel utilisation of 75% and a voltage of 0.75 V. They did not use a combustor, but that should not affect the electrical efficiency as long as preheating needs are met by recuperation. Peters et al. [43] found a similar electrical efficiency of 48% at 80% fuel utilisation and a slightly higher voltage. The analysis of Sadeghi et al. [44] resulted in a slightly higher efficiency (49.6%), but they assumed a fuel utilisation of 85% and used no inverter. Wang et al. [24] again found higher net electric efficiencies in the range of 51% to 60% using pure oxygen instead of air.

6. Conclusion

This study compared the thermodynamic performance of a marine SOFC power plant for methane, methanol, diesel, ammonia, and hydrogen. A reference model was established, which was extended with the necessary components for the different fuels. Additionally, cathode off-gas recirculation (COGR) is investigated with the purpose of improving heat regeneration. The thermodynamic model is verified with a sensitivity analysis and validated by comparing the results with thermodynamic analyses of similar SOFC systems.

The difference in electrical and heat efficiency between the fuels was significant. At a cell voltage of 0.8 V and a fuel utilisation of 80%, the highest net electrical efficiency (LHV) was found for methane (58.1%), followed by diesel (57.6%) and ammonia (55.1%). The air blower had a major influence on the net electrical efficiency, especially for low oxygen utilisation. The carbon fuels (methane, methanol, and diesel) resulted in a 15% lower power density, compared with ammonia and hydrogen. The highest heat efficiency was found for ammonia (27.4%), followed by hydrogen (25.6%). For both the methane and ammonia system, the heat quality in the exhaust was sufficient for the generation of hot water and saturated steam. Practically, this saves additional fuel or electricity for boilers.

Without COGR, the heat quality was insufficient to generate saturated steam for methanol, diesel, and hydrogen. COGR was used to increase the oxygen utilisation and thus increase the temperature in the exhaust stream. Increasing the recirculation ratio improved the heat efficiency and reduced the required heat transfer in the air pre-heater. Comparing the systems without and with COGR resulted in similar net electrical efficiencies, but the systems with COGR demonstrated a large increase the quantity and quality of the heat efficiency. This resulted in an increase in the heat efficiency of 11.9% to 105.0% for the different fuels. A smaller primary airflow also resulted in a decrease of heat transfer in the air pre-heater of 21.9% to 72.6%, reducing the size, weight, and cost of this heat exchanger.

Further research will be needed to tackle the design problems of a high-temperature cathode recirculation loop, for which low-temperature COGR or specialised high-temperature blowers are possible strategies. Nevertheless, COGR offers a promising method to increase heat recovery, improving the total efficiency of the power plant. The results of this study can be used to evaluate the fuel choice of a marine SOFC power plant and to improve heat recovery, with the overarching goal to reduce ship emissions.

CRediT authorship contribution statement

B.N. van Veldhuizen: Conceptualisation, Methodology, Formal analysis, Writing – original draft. **L. van Biert:** Conceptualisation, Methodology, Validation, Writing – review & editing. **A. Amladi:** Validation, Writing – original draft. **T. Woudstra:** Conceptualisation, Methodology, Software. **K. Visser:** Supervision. **P.V. Aravind:** Supervision.

Declaration of competing interest

The authors declare that they have no known competing financial interests or personal relationships that could have appeared to influence the work reported in this paper.

Data availability

The thermodynamic models, flowsheet data, raw simulation results and result analysis files are publised in a data repository and can be accessed via https://doi.org/10.4121/21542106.

Acknowledgement

The research is supported by the European Consortium 'Nautilus' (Grant agreement ID: 861647). The Nautilus Project aims at developing, evaluating and validating a highly efficient and dynamic integrated SOFC fuelled by LNG for long-haul passenger ships.

Appendix. Simulation parameters of used validation studies

See Tables 7 and 8.

Table 7
Comparison of SOFC system analyses without COGR. Only comparable studies are included, which means planar O^{2-} conducting SOFCs operated on atmospheric pressure. All efficiency data is based on LHV. When no stack temperature is provided, the average between stack inlet and outlet is reported.

Fuel	Reference	*SOFC operation*							*System characteristics*		*Performance*
		Reforming	Pre-reform ratio	Voltage	Current density	AOGR	Overall fuel utilisation	Stack temperature	Isentropic blower efficiency	DC/AC inverter efficiency	Net electric efficiency
		–	–	V	A/m^2	–	–	°C	–	–	–
Methane	Kazempoor et al. [26]	SR	30%	0.7	5000	✓	80%	750	73%	92%	49.5%
	Liso et al. [19]	SR	40%	?	?	–	80%	750	?	92%	61.0%
	Jia et al. [27]	SR	50%	?	?	–	85%	820	70%	98%	41.0%
	Mehr et al. [17]	SR	0%	0.62	6000	–	85%	727	85%	97%	41.8%[a]
	Ahmadi et al. [62]	SR	0%	?	5500	–	80%	640	85%	97%	47.8%
	This study	SR	20%	0.80	3483	–	80%	720	70%	96%	58.1%
	This study	SR	40%	0.80	3429	–	80%	720	70%	96%	57.7%
Methanol	Sangtongk-itcharoen et al. [63]	SR	100%	0.62	3230	–	80%	900	?	100%	45.0%
	Cocco and Tola [34]	SR	100%	?	3000	–	85%	900	82%[b]	95%	50.0%
	Leone et al. [33]	SR	100%	?	6600	–	80%	800	?	?	51.0%
	Rokni [64]	ME	100%	?	?	✓	80%	700	70%	97%	51.9%
	This study	SR	100%	0.80	3526	–	80%	720	70%	96%	48.9%
Diesel	Ezgi et al. [65]	ATR	90%	0.80	4000	–	90%	775	72%[c]	100%	55.3%
	Nehter et al. [66]	SR	100%	0.75	?	✓	73%	800	?	?	55.0%[d]
	Huerta et al. [21]	SR	100%	0.75	?	✓	85%	775	65%	?	56.0%
	This study	SR	100%	0.80	3538	–	80%	720	70%	96%	57.6%
Ammonia	Farhad and Hamdullah-pur [37]	IC	0%	0.73	?	–	80%	800	55%[e]	100%	41.0%
	Rokni [64]	IC	0%	?	?	–	80%	700	70%	97%	51.8%
	Cinti et al. [51]	IC	0%	?	?	–	80%	750	80%	100%	55.0%
	Barelli et al. [38]	IC	0%	0.78	5000	–	80%	750	90%	95%	52.1%
	Selvam et al. [67]	IC	0%	0.855	2000	–	80%	800	80%	98%	59.8%
	This study	IC	0%	0.80	4075	–	80%	720	70%	96%	55.1%
Hydrogen	Kazempoor et al. [26]	–	–	0.78	5000	–	80%	750	73%	92%	37.5%
	Botta et al. [68]	–	–	0.75	8000	–	75%	850	80%	100%	40.0%
	Peters et al. [43]	–	–	0.86	5000	–	80%	750	60%	95%	48.0%
	Sadeghi et al. [44]	–	–	0.85	10 000	–	85%	750	85%	100%	49.6%
	This study	–	–	0.80	4100	–	80%	720	70%	96%	47.1%

General: – = Not applicable, ? = Not reported by author.
Reforming: SR = Steam Reforming, ME = Methanation, ATR = Auto Thermal Reforming, IC = Internal Cracking.
AOGR = Anode Off-gas Recirculation.

[a]Net electric exergy efficiency.
[b]Polytropic efficiency.
[c]Overall efficiency.
[d]Gross energy efficiency.
[e]Overall blower efficiency.

Table 8
Comparison of SOFC system analyses with COGR. Only comparable studies are included, which means planar O^{2-} conducting SOFCs operated on atmospheric pressure. All efficiency data is based on LHV. For diesel and ammonia, no representative studies with COGR were found.

Fuel	Reference	*SOFC operation*								*System characteristics*		*Performance*
		Reforming	Pre-reform ratio	COGR type	COG RR	Voltage	Current density	Fuel utilisation	Stack temperature	Isentropic blower efficiency	DC/AC inverter efficiency	Net electric efficiency
		–	–	–	–	V	A/m^2	–	°C	–	–	–
Methane	Kazempoor et al. [26]	SR	30%	EJ	0.6	0.69	5000	80%	750	73%	92%	53.7%
	Liso et al. [19]	SR	40%	EJ	0.75	0.80	?	80%	750	?	92%	58.0%
	Jia et al. [27]	SR	0%	?	0.5	?	?	85%	820	70%	98%	51.0%
	Mehr et al. [17]	SR	0%	?	0.3	0.60	6000	85%	727	85%	97%	40.2%[a]
	Wang et al. [24]	SR	80%	BL	?	0.83	4000	90%	710	?	100%	65.9%
	This study	SR	20%	BL	0.2	0.80	3465	80%	750	70%	96%	58.0%
Methanol	Wang et al. [24]	SR	100%	BL	?	0.83	4000	90%	710	?	100%	60.2%
	This study	SR	100%	BL	0.64	0.80	3464	80%	720	70%	96%	49.5%
Hydrogen	Kazempoor et al. [26]	–	–	EJ	0.6	0.78	5000	80%	750	73%	92%	40.3%
	Wang et al. [24]	–	–	BL	?	0.859	4000	90%	710	?	100%	58.3%
	This study	–	–	BL	0.64	0.80	4039	80%	720	70%	96%	46.8%

General: – = Not applicable, ? = Not reported by author
Reforming: SR = Steam Reforming.
COGR type: BL = Air recirculation with blower, EJ = Air recirculation with ejector.
[a]Net electric exergy efficiency.

References

[1] IMO. UN body adopts climate change strategy for shipping. 2018, URL: http://www.imo.org/en/MediaCentre/PressBriefings/Pages/06GHGinitialstrategy.aspx.

[2] IMO. Marpol annex VI and NTC 2008 with guidelines for implementation. Technical report, 2013.

[3] Van Hoecke L, Laffineur L, Campe R, Perreault P, Verbruggen SW, Lenaerts S. Challenges in the use of hydrogen for maritime applications. 2021, p. 815–43. http://dx.doi.org/10.1039/d0ee01545h.

[4] International Gas Union. 2020 world LNG report. Technical Report, 2020, p. 68, URL: https://igu.org/resources/2020-world-lng-report/.

[5] Xiang L, Song E, Ding Y. A two-zone combustion model for knocking prediction of marine natural gas SI engines. In: Energies 2018, Vol. 11. Multidisciplinary Digital Publishing Institute; 2018, p. 561. http://dx.doi.org/10.3390/EN11030561, Vol. 11, Page 561. URL: https://www.mdpi.com/1996-1073/11/3/561/htmhttps://www.mdpi.com/1996-1073/11/3/561.

[6] Baldi F, Moret S, Tammi K, Maréchal F. The role of solid oxide fuel cells in future ship energy systems. Energy 2020;194:116811. http://dx.doi.org/10.1016/j.energy.2019.116811.

[7] van Biert L, Woudstra T, Godjevac M, Visser K, Aravind PV. A thermodynamic comparison of solid oxide fuel cell-combined cycles. J Power Sources 2018;397:382–96. http://dx.doi.org/10.1016/j.jpowsour.2018.07.035.

[8] Gür TM. Comprehensive review of methane conversion in solid oxide fuel cells: Prospects for efficient electricity generation from natural gas. 2016, p. 1–64. http://dx.doi.org/10.1016/j.pecs.2015.10.004.

[9] van Biert L, Godjevac M, Visser K, Aravind PV. A review of fuel cell systems for maritime applications. J Power Sources 2016;327(February 2018):345–64. http://dx.doi.org/10.1016/j.jpowsour.2016.07.007.

[10] Weber A. Fuel flexibility of solid oxide fuel cells. Fuel Cells 2021;21(5):440–52. http://dx.doi.org/10.1002/FUCE.202100037, URL: https://onlinelibrary.wiley.com/doi/full/10.1002/fuce.202100037https://onlinelibrary.wiley.com/doi/abs/10.1002/fuce.202100037https://onlinelibrary.wiley.com/doi/10.1002/fuce.202100037.

[11] Lagemann B, Lindstad E, Fagerholt K, Rialland A, Ove Erikstad S. Optimal ship lifetime fuel and power system selection. Transp Res D 2022;102:103145. http://dx.doi.org/10.1016/J.TRD.2021.103145.

[12] Hajabdollahi Z, Fu PF. Multi-objective based configuration optimization of SOFC-gt cogeneration plant. Appl Therm Eng 2017;112:549–59. http://dx.doi.org/10.1016/J.APPLTHERMALENG.2016.10.103.

[13] Sarmah P, Gogoi TK, Das R. Estimation of operating parameters of a SOFC integrated combined power cycle using differential evolution based inverse method. Appl Therm Eng 2017;119:98–107. http://dx.doi.org/10.1016/J.APPLTHERMALENG.2017.03.060.

[14] Zhang S, Liu H, Liu M, Sakaue E, Li N, Zhao Y. An efficient integration strategy for a SOFC-GT-SORC combined system with performance simulation and parametric optimization. Appl Therm Eng 2017;121:314–24. http://dx.doi.org/10.1016/J.APPLTHERMALENG.2017.04.066.

[15] Baldi F, Ahlgren F, Nguyen T, Thern M, Andersson K. Energy and exergy analysis of a cruise ship. Energies 2018;11(10):2508. http://dx.doi.org/10.3390/en11102508, URL: http://www.mdpi.com/1996-1073/11/10/2508.

[16] Klein Woud H, Stapersma D. Design of auxiliary systems shafting and flexible mounting systems. 2011.

[17] Mehr AS, Mahmoudi SMS, Yari M, Chitsaz A. Thermodynamic and exergoeconomic analysis of biogas fed solid oxide fuel cell power plants emphasizing on anode and cathode recycling: A comparative study. Energy Convers Manage 2015;105:596–606. http://dx.doi.org/10.1016/J.ENCONMAN.2015.07.085.

[18] Chen J, Li J, Zhou D, Zhang H, Weng S. Control strategy design for a SOFC-GT hybrid system equipped with anode and cathode recirculation ejectors. Appl Therm Eng 2018;132:67–79. http://dx.doi.org/10.1016/J.APPLTHERMALENG.2017.12.079.

[19] Liso V, Olesen AC, Nielsen MP, Kær SK. Performance comparison between partial oxidation and methane steam reforming processes for solid oxide fuel cell (SOFC) micro combined heat and power (CHP) system. Energy 2011;36(7):4216–26. http://dx.doi.org/10.1016/j.energy.2011.04.022.

[20] Chen J, Liang M, Zhang H, Weng S. Study on control strategy for a SOFC-GT hybrid system with anode and cathode recirculation loops. Int J Hydrogen Energy 2017;42(49):29422–32. http://dx.doi.org/10.1016/J.IJHYDENE.2017.09.165.

[21] Huerta GV, Jordán JA, Dragon M, Leites K, Kabelac S. Exergy analysis of the diesel pre-reforming solid oxide fuel cell system with anode off-gas recycling in the schibz project. Part I: Modeling and validation. Int J Hydrogen Energy 2018;43(34):16684–93. http://dx.doi.org/10.1016/j.ijhydene.2018.04.216.

[22] Hollmann J, Fuchs M, Spieker C, Gardemann U, Steffen M, Luo X, Kabelac S. System simulation and analysis of an LNG-fueled SOFC system using additively manufactured high temperature heat exchangers. Energies 2022;15(3):941. http://dx.doi.org/10.3390/EN15030941, URL: https://www.mdpi.com/1996-1073/15/3/941/htmhttps://www.mdpi.com/1996-1073/15/3/941.

[23] Tomberg M, Heddrich MP, Metten M, Ansar SA, Friedrich KA. Operation of a solid oxide fuel cell reactor with multiple stacks in a pressured system with fuel gas recirculation. Energy Technol 2022;2101075. http://dx.doi.org/10.1002/ENTE.202101075, URL: https://onlinelibrary-wiley-com.tudelft.idm.oclc.org/doi/full/10.1002/ente.202101075https://onlinelibrary-wiley-com.tudelft.idm.oclc.org/doi/abs/10.1002/ente.202101075https://onlinelibrary-wiley-com.tudelft.idm.oclc.org/doi/10.1002/ente.202101075.

[24] Wang L, Zhang Y, Pérez-Fortes M, Aubin P, Lin TE, Yang Y, Maréchal F, Van herle J. Reversible solid-oxide cell stack based power-to-x-to-power systems: Comparison of thermodynamic performance. Appl Energy 2020;275:115330. http://dx.doi.org/10.1016/J.APENERGY.2020.115330.

[25] van Biert L, Visser K, Aravind PV. A comparison of steam reforming concepts in solid oxide fuel cell systems. Appl Energy 2020;264:114748. http://dx.doi.org/10.1016/J.APENERGY.2020.114748.
[26] Kazempoor P, Dorer V, Ommi F. Evaluation of hydrogen and methane-fuelled solid oxide fuel cell systems for residential applications: System design alternative and parameter study. Int J Hydrogen Energy 2009;34:8630–44. http://dx.doi.org/10.1016/j.ijhydene.2009.07.119.
[27] Jia J, Li Q, Luo M, Wei L, Abudula A. Effects of gas recycle on performance of solid oxide fuel cell power systems. Energy 2011;36(2):1068–75. http://dx.doi.org/10.1016/j.energy.2010.12.001.
[28] van Veldhuizen BN, Amladi A, van Biert L. Genset performance with future fuels. Technical report, Nautilus Project; 2021.
[29] Geneidy RE, Otto K, Ahtila P, Kujala P, Sillanpää K, Mäki-Jouppila T. Increasing energy efficiency in passenger ships by novel energy conservation measures. J Mar Eng Technol 2018;17(2):85–98. http://dx.doi.org/10.1080/20464177.2017.1317430, URL: https://www.tandfonline.com/action/journalInformation?journalCode=tmar20.
[30] Stiller C. Design, operation and control modelling of SOFC/GT hybrid systems. Technical report, Trondheim: Norwegian University of Science and Technology; 2006, URL: https://ntnuopen.ntnu.no/ntnu-xmlui/handle/11250/231300.
[31] Xu Q, Ni M. Modelling of high temperature direct methanol solid oxide fuel cells. Int J Energy Res 2021;45(2):3097–112. http://dx.doi.org/10.1002/er.6003.
[32] Laosiripojana N, Assabumrungrat S. Catalytic steam reforming of methane, methanol, and ethanol over Ni/YSZ: The possible use of these fuels in internal reforming SOFC. J Power Sources 2007;163(2):943–51. http://dx.doi.org/10.1016/j.jpowsour.2006.10.006.
[33] Leone P, Lanzini A, Ortigoza-Villalba GA, Borchiellini R. Operation of a solid oxide fuel cell under direct internal reforming of liquid fuels. Chem Eng J 2012;191:349–55. http://dx.doi.org/10.1016/J.CEJ.2012.03.030.
[34] Cocco D, Tola V. Externally reformed solid oxide fuel cell-micro-gas turbine (SOFC-MGT) hybrid systems fueled by methanol and di-methyl-ether (DME). Energy 2009;34(12):2124–30. http://dx.doi.org/10.1016/j.energy.2008.09.013.
[35] Ahmed S, Krumpelt M. Hydrogen from hydrocarbon fuels for fuel cells. Int J Hydrogen Energy 2001;26(4):291–301. http://dx.doi.org/10.1016/S0360-3199(00)00097-5.
[36] Papadias D, Lee SHD, Chmielewski DJ. Autothermal reforming of gasoline for fuel cell applications: A transient reactor model. Ind Eng Chem Res 2006;45:5841–58. http://dx.doi.org/10.1021/ie051291t.
[37] Farhad S, Hamdullahpur F. Conceptual design of a novel ammonia-fuelled portable solid oxide fuel cell system. J Power Sources 2010;195(10):3084–90. http://dx.doi.org/10.1016/J.JPOWSOUR.2009.11.115.
[38] Barelli L, Bidini G, Cinti G. Operation of a solid oxide fuel cell based power system with ammonia as a fuel: Experimental test and system design. Energies 2020;13(23). http://dx.doi.org/10.3390/en13236173.
[39] Cinti G, Desideri U, Penchini D, Discepoli G. Experimental analysis of SOFC fuelled by ammonia. Fuel Cells 2014;14(2):221–30. http://dx.doi.org/10.1002/FUCE.201300276, URL: https://onlinelibrary-wiley-com.tudelft.idm.oclc.org/doi/full/10.1002/fuce.201300276https://onlinelibrary-wiley-com.tudelft.idm.oclc.org/doi/abs/10.1002/fuce.201300276https://onlinelibrary-wiley-com.tudelft.idm.oclc.org/doi/10.1002/fuce.201300276.
[40] Ilbas M, Asmare Alemu M, Mustafa Cimen F. Comparative performance analysis of a direct ammonia-fuelled anode supported flat tubular solid oxide fuel cell: A 3D numerical study. Int J Hydrogen Energy 2022;47:3416–28. http://dx.doi.org/10.1016/j.ijhydene.2021.10.080, URL: www.sciencedirect.com.
[41] Stoeckl B, Subotić V, Preininger M, Schwaiger M, Evic N, Schroettner H, Hochenauer C. Characterization and performance evaluation of ammonia as fuel for solid oxide fuel cells with Ni/YSZ anodes. Electrochim Acta 2019;298:874–83. http://dx.doi.org/10.1016/J.ELECTACTA.2018.12.065.
[42] Saadabadi SA, Thallam Thattai A, Fan L, Lindeboom REF, Spanjers H, Aravind PV. Solid oxide fuel cells fuelled with biogas: Potential and constraints. 2019, p. 194–214. http://dx.doi.org/10.1016/j.renene.2018.11.028.
[43] Peters R, Deja R, Engelbracht M, Frank M, Nguyen VN, Blum L, Stolten D. Efficiency analysis of a hydrogen-fueled solid oxide fuel cell system with anode off-gas recirculation. J Power Sources 2016;328:105–13. http://dx.doi.org/10.1016/j.jpowsour.2016.08.002.
[44] Sadeghi M, Jafari M, Hajimolana YS, Woudstra T, Aravind PV. Size and exergy assessment of solid oxide fuel cell-based H2-fed power generation system with alternative electrolytes: A comparative study. Energy Convers Manage 2021;228:113681. http://dx.doi.org/10.1016/J.ENCONMAN.2020.113681.
[45] Aravind PV, Woudstra T, Woudstra N, Spliethoff H. Thermodynamic evaluation of small-scale systems with biomass gasifiers, solid oxide fuel cells with Ni/GDC anodes and gas turbines. J Power Sources 2009;190(2):461–75. http://dx.doi.org/10.1016/J.JPOWSOUR.2009.01.017.
[46] Bae Y, Lee S, Yoon KJ, Lee JH, Hong J. Three-dimensional dynamic modeling and transport analysis of solid oxide fuel cells under electrical load change. Energy Convers Manage 2018;165:405–18. http://dx.doi.org/10.1016/J.ENCONMAN.2018.03.064.
[47] CAGI. Compressed air and gas institute. 2022, URL: https://www.cagi.org/education/glossary.aspx.
[48] Peters R, Deja R, Blum L, Pennanen J, Kiviaho J, Hakala T. Analysis of solid oxide fuel cell system concepts with anode recycling. Int J Hydrogen Energy 2013;38(16):6809–20. http://dx.doi.org/10.1016/j.ijhydene.2013.03.110.
[49] Ni M, Leung DYC, Leung MKH. Thermodynamic analysis of ammonia fed solid oxide fuel cells: Comparison between proton-conducting electrolyte and oxygen ion-conducting electrolyte. J Power Sources 2008;183(2):682–6. http://dx.doi.org/10.1016/j.jpowsour.2008.05.022.
[50] Mori Y, Sheindlin AE, Afgan NH. High temperature heat exchangers. J Pressure Vessel Technol 1987;109(2):264. http://dx.doi.org/10.1115/1.3264915.
[51] Cinti G, Discepoli G, Sisani E, Desideri U. SOFC operating with ammonia: Stack test and system analysis. Int J Hydrogen Energy 2016;41(31):13583–90. http://dx.doi.org/10.1016/J.IJHYDENE.2016.06.070.
[52] Lienhard J. A heat transfer textbook. 5th ed.. Cambridge Massachusetts: Phlogiston Press; 2019.
[53] van Biert L, Godjevac M, Visser K, Aravind PV. Dynamic modelling of a direct internal reforming solid oxide fuel cell stack based on single cell experiments. Appl Energy 2019;250:976–90. http://dx.doi.org/10.1016/J.APENERGY.2019.05.053.
[54] Arsalis A. Thermoeconomic modeling and parametric study of hybrid SOFC-gas turbine-steam turbine power plants ranging from 1.5 to 10 MWe. J Power Sources 2008;181(2):313–26. http://dx.doi.org/10.1016/j.jpowsour.2007.11.104.
[55] Fontell E, Kivisaari T, Christiansen N, Hansen JB, Pålsson J. Conceptual study of a 250 kW planar SOFC system for CHP application. J Power Sources 2004;131(1–2):49–56. http://dx.doi.org/10.1016/j.jpowsour.2004.01.025.
[56] Becker WL, Braun RJ, Penev M, Melaina M. Design and technoeconomic performance analysis of a 1 MW solid oxide fuel cell polygeneration system for combined production of heat, hydrogen, and power. J Power Sources 2012;200:34–44. http://dx.doi.org/10.1016/j.jpowsour.2011.10.040.
[57] Bakalis DP, Stamatis AG. Incorporating available micro gas turbines and fuel cell: Matching considerations and performance evaluation. Appl Energy 2013;103:607–17. http://dx.doi.org/10.1016/j.apenergy.2012.10.026.
[58] Tan L, Yang C, Zhou N. Synthesis/design optimization of SOFC-PEM hybrid system under uncertainty. Chin J Chem Eng 2015;23(1):128–37. http://dx.doi.org/10.1016/j.cjche.2014.09.040.
[59] Sargent RG. Verification and validation of simulation models. In: Proceedings - winter simulation conference. 2010, p. 166–83. http://dx.doi.org/10.1109/WSC.2010.5679166.
[60] Payne R, Love J, Kah M. Generating electricity at 60% electrical efficiency from 1-2 kWe SOFC products. In: ECS transactions. The Electrochemical Society; 2009, p. 231–9. http://dx.doi.org/10.1149/1.3205530.
[61] Chen J, Chen Y, Zhang H, Weng S. Effect of different operating strategies for a SOFC-GT hybrid system equipped with anode and cathode ejectors. Energy 2018;163:1–14. http://dx.doi.org/10.1016/J.ENERGY.2018.08.032.
[62] Ahmadi S, Ghaebi H, Shokri A. A comprehensive thermodynamic analysis of a novel CHP system based on SOFC and APC cycles. Energy 2019;186:115899. http://dx.doi.org/10.1016/J.ENERGY.2019.115899.
[63] Sangtongkitcharoen W, Vivanpatarakij S, Laosiripojana N, Arpornwichanop A, Assabumrungrat S. Performance analysis of methanol-fueled solid oxide fuel cell system incorporated with palladium membrane reactor. Chem Eng J 2008;138(1–3):436–41. http://dx.doi.org/10.1016/J.CEJ.2007.06.021.
[64] Rokni M. Thermodynamic analysis of SOFC (solid oxide fuel cell)-stirling hybrid plants using alternative fuels. Energy 2013;61:87–97. http://dx.doi.org/10.1016/j.energy.2013.06.001.
[65] Ezgi C, Çoban MT, Selvi O. Design and thermodynamic analysis of an SOFC system for naval surface ship application. J Fuel Cell Sci Technol 2013;10(3). http://dx.doi.org/10.1115/1.4024254, URL: http://asmedigitalcollection.asme.org/electrochemical/article-pdf/10/3/031006/6129726/fc_10_3_031006.pdf.
[66] Nehter P, Wildrath B, Bauschulte A, Leites K. Diesel based SOFC demonstrator for maritime applications. ECS Trans 2017;78(1):171–80. http://dx.doi.org/10.1149/07801.0171ecst.
[67] Selvam K, Komatsu Y, Sciazko A, Kaneko S, Shikazono N. Thermodynamic analysis of 100% system fuel utilization solid oxide fuel cell (SOFC) system fueled with ammonia. Energy Convers Manage 2021;249:114839. http://dx.doi.org/10.1016/J.ENCONMAN.2021.114839.
[68] Botta G, Patel HC, Sebastiani F, Aravind PV. Thermodynamic and exergy analysis of reversible solid oxide cell systems. ECS Trans 2015;68(1):3265–77. http://dx.doi.org/10.1149/06801.3265ECST/XML, URL: https://iopscience.iop.org/article/10.1149/06801.3265ecsthttps://iopscience.iop.org/article/10.1149/06801.3265ecst/meta.